

On the ballistic response of comminuted ceramics

A Hameed¹, G J Appleby-Thomas^{1,*}, D C Wood¹, P J Hazell² and K M Jaansalu³

¹Cranfield University, Shrivenham, Swindon, SN6 8LA, UK

²The University of New South Wales, UNSW Canberra, Northcott Drive, Canberra, ACT 2600, Australia

³Royal Military College of Canada, Ontario, Canada

*E-mail: g.applebythomas@cranfield.ac.uk

Abstract. Recent results have strongly suggested that the ballistic-resistance of different comminuted ceramics is similar, independent of the original strength of the material. In particular, experimental work focused on the ballistic response of such materials has suggested that ballistic response is largely controlled by shattered material morphology. Consequently, it has been postulated that control of the nature of ceramic fragmentation should provide a potential route to optimise post-impact ballistic resistance. In particular, such an approach would open up a route to control in multi-hit capabilities. Here, ballistic tests into pre-formed ‘fragmented-ceramic’ analogues assembled from compacted alumina powders with two differing morphologies were conducted. Strong hints of a morphology-based contribution to ballistic resistance were apparent, although there was insufficient fidelity in the experimental data set to categorically identify the nature of this contribution.

1. Introduction

High hardness and low density have led to ceramic materials playing an important role in armour applications [1, 2]. When a projectile impacts a target it will impart a compressive impulse to the material; however on reaching a free surface or an interface with a material of lower impedance, such a compressive wave will be reflected as a tensile pulse – putting the target into tension. This initial compressive wave will fracture the ceramic – meaning that the slower-moving penetrator is always moving into pre-damaged material [2]. Penetration of a ceramic armour joined to a backing material can involve up to four stages [1]: (1) overmatch –leading to surface-defeat (dwell); (2) initial penetration – once a cone of comminuted (crushed) material forms ahead of the projectile it begins to penetrate, potentially whilst possibly still undergoing dwell, with the steadily decreasing size of the comminuted material increasing pressure both on the backing and radially; (3) backing flexure, before; (4) failure of the backing layer – typically via plugging or similar. Inherent flaws within ceramic materials (e.g. pores, micro cracks and grain boundaries) lead to their brittle nature and act as stress concentrators during both compressive and tensile loading. While crack propagation will be inhibited during initial compressive loading, arrival of tensile releases provides an opportunity for micro fracture to occur, leading to material failure [3]. While strength rapidly decreases during the initial



penetration phase, several studies which have shown that, on further compaction, the resultant comminuted material then provides a residual resisting strength [4-6].

Holmquist et al. [7] studied such behaviour, at the defeat mechanisms for SiC tiles impacted (in a reverse ballistics configuration) by l/d 70, 1-mm diameter Au long rods. Flash X-ray analysis showed a non-linear penetration velocity in all cases, in line with computational simulations. This behaviour was attributed to the multi-phased nature of the ceramic failure – with impacted material being comminuted before penetration occurred. However, the nature of this comminuted material, along with its precise contribution to ballistic resistance, was not discussed.

Horsfall et al. [8] investigated the ballistic response of fractured materials via a series of depth-of-penetration (DOP) tests using 7.62 mm FFV rounds (c.a. 950 m/s). Varying thicknesses of explosively comminuted Sintox® FA (95% alumina) tiles and cold-pressed 67% dense 80- μ m grain size alumina compacts were confined within steel frames, with DOP into backing aluminium plates measured post-impact and compared to the response of intact material. While ballistic resistance was reduced, the shattered material still provided a significant resistance to penetration, shattering the core – whereas the pressed material had a less marked effect. The reduced performance of the powder compacts was tentatively attributed by the authors to both a relative lack of confinement and – more significantly – the fact that the pressed powder had a spherical morphology which would have minimised frictional effects during compression. It was suggested that this difference in morphology might be partially responsible for the enhanced behaviour of the shattered tiles which possessed an angular microstructure; further, it was pointed out that the shattered tiles are analogous to the state which the intact tiles would enter shortly after impact. Similar work by Nandal et al. [4] employed an identical confinement rig to explosively shatter and test via DOP a variety of different ceramic materials (Sintox® FA - alumina, EkasticT and PS-500 – both SiC). Little difference in the subsequent effective ballistic efficiency (E_m ; see equation (a) later) was apparent, despite substantially different initial strengths. Differing explosive loads were used to shatter the alumina and the two SiC grades respectively. However, in line with the results from references [7] and [8], the relative independence of E_m from material type was taken to suggest that the ballistic resistance provided by the shattered material was dependant on the form of the particles (morphology), rather than material strengths. While arguably a reasonable conclusion as all three materials were shattered in a similar manner, no systematic study of the effects of this explosive loading on microstructure was undertaken.

Despite such studies suggesting comminuted material controls penetration into ceramics, there is a relative paucity of data on the influence of comminuted microstructure. Several authors [4, 7, 9] have postulated that microstructure plays a key role, with Horsfall et al. [8] actively selecting the microstructure via cold pressing. Here, penetration of partially-stripped FFV rounds into cold-pressed alumina compacts with two differing morphologies has been studied. The commercially available alumina powders had both spherical and angular morphologies. In line with other studies [4, 8] the depth-of-penetration technique [1, 10, 11] has then been employed to allow the ballistic resistance displayed by each of these systems to be quantified.

2. Experimental setup

Saboted 7.62-mm FFV (WC-Co cored) rounds with the jacket removed from the tip, to provide a consistent target material in case of latter simulation, were launched into the target compacts at 899 ± 3 m/s (measured via high speed camera) using a 30-mm bore, 5-m barrel, single-stage gas-gun. Targets compacts comprised commercially-sourced plasma spray Al_2O_3 powders cold pressed in-situ in 36-mm deep, 70-mm diameter hollow dural cylinder with a 6-mm thick end section and internal 50-mm internal diameter. This puck was pre-filled to a set depth with the chosen powder before pressing to 10, 30 or 70 tonnes; the cold compact was then sealed in place with an epoxy resin before the surrounding edges of the Al cup were machined flush with the encapsulated compact. This arrangement, shown in figure 1, was then epoxied to the outer face of a series of 4 Al 6082 witness plates, with the 6-mm thick cylinder front face forming the outer target facing.

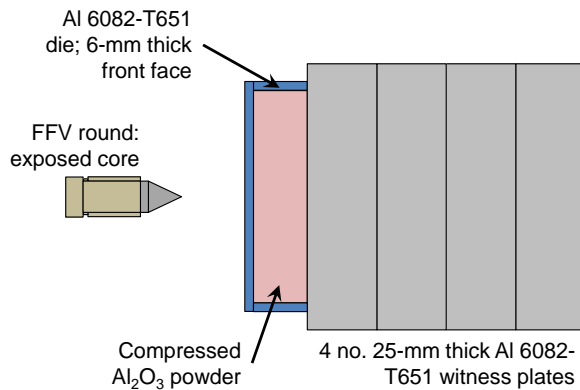
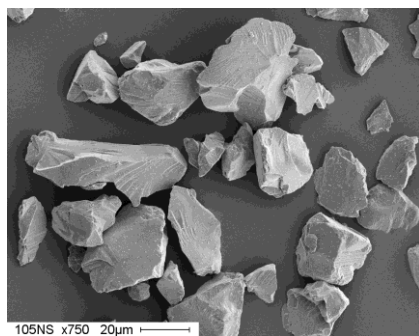
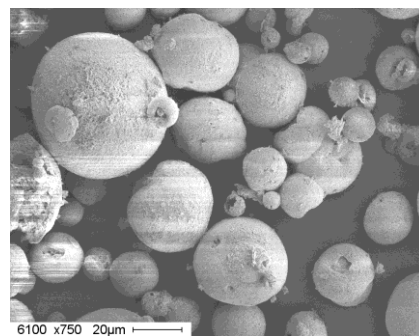


Figure 1. Experimental setup, showing cold-pressed powder compact adhered to backing Al 6082 witness plates.

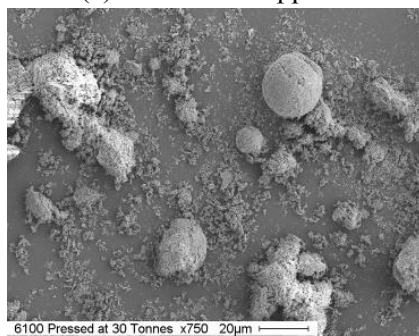
Two differing powders were employed, both manufactured by Sulzer Metco™, namely Metco 105NS and 6100. As shown in figures 2(a) and (b) respectively, these possessed angular and spherical morphologies. On pressing little difference beyond some rounding of particle edges was apparent with the 105NS material. However, as shown in figures 2(c) and (d), the spherical 6100 material gradually compressed to a laminar structure at 30 and 70 tonnes respectively.



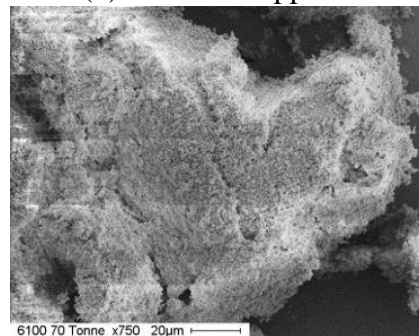
(a) 105NS: as-supplied



(b) 6100: as-supplied



(c) 6100: pressed to 30 tonnes



(d) 6100 pressed to 70 tonnes

Figure 2. Scanning electron micrographs of Sulzer Metco Al₂O₃ powders.

3. Results and discussion

Twelve DOP experiments were conducted; two test on each combination of powder type and pressing weight. Measurement of post-pressing powder thickness allowed calculation for each puck of the pressed volume (thickness $\times \pi \times [25 \text{ mm}]^2$) and, in turn, areal density (thickness \times pressed density). Final depths-of-penetration were measured by sectioning the backing Al 6082 plates which the incident projectile had penetrated (this also allowed account to be taken of any slight perturbations in the projectile path). In addition a single shot was conducted into a cover plus Al backing only – with

the measured DOP in-line with those measured under similar impact conditions elsewhere [11]. Key experimental data is presented in table 1, along with two calculated measures of ballistic efficiency, E_m [10, 12] and η [1], following equations (1) and (2) respectively.

Table 1. Key experimental results.

	Pressing weight (tonnes)	V_{impact} (m/s)	Pressed thickness (mm) / ρ (g/cc)	DOP (mm):	E_m / η
Cover + Al only	-----	899	-----	52.65	1.000 / -----
105NS	10	901	9.17 / 2.22	45.26	1.002 / 7.04
	10	898	9.01 / 2.21	44.14	1.025 / 7.06
	30	894	8.56 / 2.38	44.29	1.019 / 6.92
	30	903	8.49 / 2.43	43.36	1.034 / 6.70
	70	901	8.39 / 2.47	43.93	1.023 / 6.74
	70	894	8.24 / 2.46	43.07	1.042 / 6.79
6100	10	897	8.30 / 1.57	46.79	1.021 / 11.37
	10	899	8.56 / 1.49	48.96	0.985 / 12.04
	30	899	7.14 / 1.84	45.97	1.035 / 11.07
	30	899	7.16 / 1.80	46.08	1.035 / 11.31
	70	902	4.16 / 3.09	46.99	1.019 / 11.54
	70	897	4.28 / 2.91	46.00	1.039 / 11.70

$$E_m = \frac{\rho_{\text{Al}} P_{\text{Al-only}}}{\rho_0 t_{\text{compact}} + \rho_{\text{Al}} (P_r + t_{\text{cover}})} \quad (1)$$

$$\eta = \frac{\rho_{\text{areal}}^{\text{Al}}}{\rho_{\text{areal}}^{\text{Ceramic}}} = \frac{\rho_{\text{Al}} (P_r + t_{\text{cover}})}{\rho_0 t_{\text{compact}}} \quad (2)$$

Where: ρ_{Al} and ρ_0 are the density of the Al plates employed and the as-pressed powder compact; $P_{\text{Al-only}}$ and P_r are the penetration into the backing plate (plus cover) in the Al-only case and the residual penetration when a ceramic compact was included, and; t_{compact} and t_{cover} are the thicknesses of the as-pressed compact and the Al cover, respectively.

Measured DOP's in table 1 appear to decrease with pressing load and to be generally lower for the angular 105NS material as opposed to the spherical 6100 material; this is reflected in figure 4. However, measured DOP does not account for the ballistic resistance offered by the cover/backing materials, or differences in pressed density. The measures of E_m (effective ballistic efficiency)' and η (ballistic efficiency) detailed in equations (1) and (2) take both these factors into account.

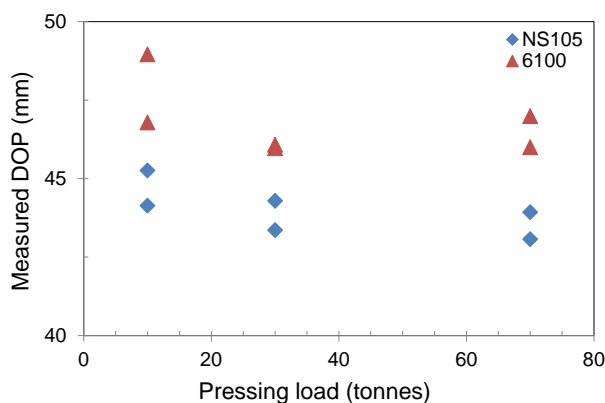


Figure 4. Variation of measured depth-of-penetration with pressing load.

Equation (1) is a rigorous measure of ‘effective’ ballistic efficiency, scaling the areal density of backing and cover material only penetrated (on the numerator) against the areal density of material required to stop the round when by a given combination ceramic was employed (on the denominator). It is immediately apparent from table 1 that E_m is relatively independent of ceramic type/pressing load. While values are nominally above unity (indicative of a slight increase in performance due to the inclusion of a ceramic layer), there is no discernible pattern differentiating the two ceramic types. This is not surprising, however, as equation (1) includes measures of the backing material areal density on both the numerator and denominator. As the ‘pre-comminuted’ ceramics employed here will have had only a small contribution to ballistic resistance [8].

Unlike E_m , the ballistic efficiency factor η is a simple ratio of the areal density of cover/backing material penetrated and ceramic compact presented in a given shot. Consequently, while not providing an absolute measure of ballistic efficiency (as no comparison is made to the baseline configuration), if employed with care it does provide a ready means of scaling between different ceramic/backing configurations. The variation of η with pressing load is shown in figure 5.

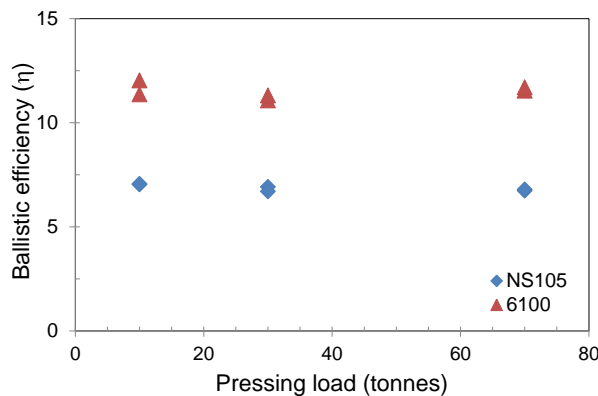


Figure 5. Variation of ballistic efficiency as defined in equation (2) with pressing load.

Equation (2) indicates that less ballistically efficient armour systems will have lower values of η due to higher resultant penetration into the backing material (a factor which dominates in the cases considered here). Consequently, Figure 5 again shows an enhanced performance for the 105NS material versus the spherical 6100. While there is a slight scatter in the 6100 data at the lowest pressing load, this disappears at elevated pressing loads (likely due to rapid removal of internal free space as the spheradised powder is compressed). Overall, while there are hints of a slight decrease in η with impact stress in both cases – potentially reflecting structural damage to the powder grains as elevated pressing loads – this behaviour sits within experimental scatter. Consequently, figure 5 appears to suggest that after initial compression there is relatively little change in ballistic performance in each case – but that the 105NS powder is measurably more effective than the 6100 one. Given that chemically identical powders were employed and that calculation of η normalises for pressed density and the areal density of cover/backing plate material penetrated, despite the low number of tests undertaken, this result appears to provide tentative evidence that particle morphology does have an influence on ballistic efficiency.

4. Conclusions

A series of depth-of-penetration tests have been carried out on a variety of cold-pressed alumina ‘pucks’. These powder compacts were designed to simulate pre-fragmented ceramic armour tiles. While the pressing weight appeared to have relatively little influence on the final ballistic properties, initial particle morphology did appear to influence ballistic response. In particular, compacts comprised of particles with an angular morphology (105NS) appeared to provide enhanced ballistic efficiency compared to spherised constituent particles; likely due to enhanced frictional effects. While

necessarily a tentative conclusion given the relatively small number of tests conducted here, this result appears to lend credence to the suggestions elsewhere in the literature that ballistic performance of fragmented ceramics is closely linked to resultant material morphology.

Acknowledgements

The experimental work reported here was undertaken during the Explosives Ordnance Engineering MSc project of Lt. Cdr. Steven Toone at Cranfield University's Shrivenham Campus.

References

- [1] Walley S M 2010 *Adv. Appl. Ceram.* **109** 446
- [2] Sternberg J 1989 *J. Appl. Phys.* **65** 3417
- [3] Antoun T, Seaman L, Curran D R, Kanel G I, Razorenov S V and Utkin A V *Spall Fracture* (New York: Springer-Verlag), pp. 162-168
- [4] Nanda H, Appleby-Thomas G J, Wood D C and Hazell P 2010 *Adv. Appl. Ceram.* **110** 286
- [5] Hazell P J and Appleby-Thomas G J 2012 *Adv. Appl. Ceram.* **111** 171
- [6] Bourne N K 2010 *Adv. Appl. Ceram.* **109** 480
- [7] Holmquist T M, Anderson Jr C E, Behner T and Orphal D L 2010 *Adv. Appl. Ceram.* **109** 467
- [8] Horsfall I, Edwards M R and Hallas M J 2010 *Adv. Appl. Ceram.* **109** 498
- [9] Bourne N K 2010 *Adv. Appl. Ceram.* **109** 480
- [10] Hazell P J 2006 *Ceramic Armour: Design and Defeat Mechanisms* (Argos Press)
- [11] Hazell P J 2010 *Adv. Appl. Ceram.* **109** 504
- [12] Rosenberg Z, Yeshurun Y and Tsaliah J 1990 *Proc. of the 12th Int. Symp. on Ballistics* vol 3 (San Antonio: Texas, USA) p. 197